Journal of Experimental Botany, Vol. 63, No. 3, pp. 1445–1459, 2012
doi:10.1093/jxb/err386 Advance Access publication 3 December, 2011
This paper is available online free of all access charges (see http://jxb.oxfordjournals.org/open_access.html for further details)

Journal of Experimental Botany
www.jxb.oxfordjournals.org

RESEARCH PAPER

Multiple strategies to prevent oxidative stress in *Arabidopsis* plants lacking the malate valve enzyme NADP-malate dehydrogenase

Inga Hebbelmann[1,*,†], Jennifer Selinski[1,†], Corinna Wehmeyer[1], Tatjana Goss[1], Ingo Voss[1], Paula Mulo[2], Saijaliisa Kangasjärvi[2], Eva-Mari Aro[2], Marie-Luise Oelze[3], Karl-Josef Dietz[3], Adriano Nunes-Nesi[4,‡], Phuc T. Do[4], Alisdair R. Fernie[4], Sai K. Talla[5], Agepati S. Raghavendra[1,5], Vera Linke[1] and Renate Scheibe[1,§]

[1] Department of Plant Physiology, FB5, University of Osnabrueck, D-49069 Osnabrueck, Germany
[2] Molecular Plant Biology, Department of Biochemistry and Food Chemistry, University of Turku, FIN-20014 Turku, Finland
[3] Biochemistry and Physiology of Plants, University of Bielefeld, D-33501 Bielefeld, Germany
[4] Max Planck Institute for Molecular Plant Physiology, Am Mühlenberg 1, D-14476 Potsdam-Golm, Germany
[5] Department of Plant Sciences, School of Life Sciences, University of Hyderabad, Hyderabad 500 046, India

* Present address: Biology Department, Brookhaven National Laboratory, Upton, NY 11973, USA.
† These authors contributed equally to this work.
‡ Present address: Max-Planck Partner Group, Departamento de Biologia Vegetal, Universidade Federal de Viçosa, Viçosa, Minas Gerais, Brazil.
§ To whom correspondence should be addressed. E-mail: scheibe@biologie.uni-osnabrueck.de

Received 12 May 2011; Revised 1 November 2011; Accepted 2 November 2011

Abstract

The nuclear-encoded chloroplast NADP-dependent malate dehydrogenase (NADP-MDH) is a key enzyme controlling the malate valve, to allow the indirect export of reducing equivalents. *Arabidopsis thaliana* (L.) Heynh. T-DNA insertion mutants of *NADP-MDH* were used to assess the role of the light-activated NADP-MDH in a typical C_3 plant. Surprisingly, even when exposed to high-light conditions in short days, *nadp-mdh* knockout mutants were phenotypically indistinguishable from the wild type. The photosynthetic performance and typical antioxidative systems, such as the Beck–Halliwell–Asada pathway, were barely affected in the mutants in response to high-light treatment. The reactive oxygen species levels remained low, indicating the apparent absence of oxidative stress, in the mutants. Further analysis revealed a novel combination of compensatory mechanisms in order to maintain redox homeostasis in the *nadp-mdh* plants under high-light conditions, particularly an increase in the NTRC/2-Cys peroxiredoxin (Prx) system in chloroplasts. There were indications of adjustments in extra-chloroplastic components of photorespiration and proline levels, which all could dissipate excess reducing equivalents, sustain photosynthesis, and prevent photoinhibition in *nadp-mdh* knockout plants. Such metabolic flexibility suggests that the malate valve acts in concert with other NADPH-consuming reactions to maintain a balanced redox state during photosynthesis under high-light stress in wild-type plants.

Key words: Malate valve, NADP-malate dehydrogenase, oxidative stress, poising mechanisms, redox homeostasis.

Introduction

Malate dehydrogenases catalyse the reversible conversion of oxaloacetate to malate using either NAD/H or NADP/H as oxidant/reductant, respectively. Additionally, these enzymes can indirectly function as a pacemaker of the transport of

Abbreviations: AAN, aminoacetonitrile; AOX, alternative oxidase; APX, ascorbate peroxidase; DHAR, dehydroascorbate reductase; GDC, glycine decarboxylase; GHA, glycine hydroxamate; GL, growth light; GR, glutathione reductase; HL, high light; MDAR, monodehydroascorbate reductase; NADP-MDH, NADP-dependent malate dehydrogenase; NPQ, non-photochemical quenching; NTRC, chloroplast NADPH-thioredoxin reductase; Prx, peroxiredoxin; qP, photochemical quenching; SHAM, salicylhydroxamic acid.

reducing equivalents between subcellular compartments, in cooperation with the membrane-bound dicarboxylate transporters. NAD-dependent isoforms of MDH are present in mitochondria, peroxisomes, cytosol, and plastids. Chloroplasts additionally possess an NADP-malate dehydrogenase (NADP-MDH) with distinct regulatory properties. This nuclear-encoded NADP-MDH is the key enzyme of the malate valve (Scheibe, 2004). NADP-MDH converts oxaloacetate to malate using NADPH, facilitating the regeneration of the electron acceptor $NADP^+$ in the chloroplasts, particularly when CO_2 assimilation is restricted.

The malate valve is suggested to balance the ATP/NADPH ratio of the chloroplast as required by changing metabolic demands (Scheibe, 2004). Export of reducing equivalents, however, needs to be well controlled in order to avoid any imbalance or depletion of chloroplast energy carriers. The reductive activation of NADP-MDH is inhibited when the NADP/NADP(H) ratio is high (Scheibe and Jacquot, 1983; Faske *et al.*, 1995). The activation of NADP-MDH, and consequently the rate of malate export from the chloroplast, is high, only when there is a shortage of $NADP^+$. The activation state of NADP-MDH changes within seconds to minutes, due to this post-translational regulatory mechanism. Thus, the enzyme appears to play an important role in the short-term adjustment of the stromal NADP(H) redox state in response to changing environmental conditions, so as to ensure the maintenance of redox homeostasis (Scheibe *et al.*, 2005).

Knockout mutants of *Arabidopsis thaliana* (L.) Heynh. (*nadp-mdh*) deficient in NADP-MDH activity were used to assess the role of the light-activated NADP-MDH in C_3 plants. Molecular and biochemical analyses of these plants grown in or transferred to challenging high-light (HL) conditions were conducted to understand potential compensatory mechanisms that counteract redox imbalances and oxidative stress. Amongst these systems are the NTRC/2-Cys peroxiredoxin (Prx) system in chloroplasts (Serrato *et al.*, 2004; Pérez-Ruiz *et al.*, 2006), other antioxidant enzymes and low molecular weight antioxidants in different cellular compartments (Foyer and Noctor, 2009), photorespiration (Wingler *et al.*, 2000; Igamberdiev *et al.*, 2001), and even the mitochondrial alternative oxidase (AOX) pathway (Yoshida *et al.*, 2007; Strodtkötter *et al.*, 2009). The detailed analysis presented here revealed that the *nadp-mdh* mutants employed a combination of multiple strategies to counteract the oxidative stress, and protect the chloroplasts from photoinhibition under HL.

Materials and methods

Growth of plant material

Wild-type (WT) and transgenic *Arabidopsis thaliana* (L.) Heynh. (ecotype Columbia) plants were cultivated in a growth chamber in soil under short-day conditions with a 7.5 h daily light period, a light intensity of 50 µmol quanta m^{-2} s^{-1}, and a temperature of 20 °C. These conditions are defined as growth light (GL). To apply stress conditions, plants were exposed to HL (750 µmol quanta m^{-2} s^{-1}) for 7 h or for alternative periods as indicated. To analyse plant growth in early stages, single seeds were placed in pots in soil, and plants were grown under short-day conditions at a light intensity of 150 µmol quanta m^{-2} s^{-1} for 5 weeks. Then the fresh and dry weight of the above-ground biomass was determined in 100 seedlings of each genotype.

For growth analyses, single seeds were planted in Petri dishes on agar. The nutrient medium described by Wilson *et al.* (1990) was used with some modifications. The medium contained 2.5 mM KCl, 1.25 mM KH_2PO_4, 1 mM $MgSO_4$, 2 mM $CaCl_2$, 80 µM Fe-EDTA, 24 µM H_3BO_3, 4 µM $MnCl_2$, 0.2 µM $CuSO_4$, 0.4 µM $ZnSO_4$, 0.6 µM Na_2MoO_4, and 0.8% agar *pro analysi* (Carl Roth, Karlsruhe, Germany). The pH was adjusted to 5.7 with KOH, and the medium was supplemented with 1.8 mM nitrate. For uniform germination, the plates were initially incubated for 2 d in the dark at 4 °C. Seedlings were grown under sterile conditions. After 4 weeks of growth under short-day conditions at 150 µmol quanta m^{-2} s^{-1}, the fresh weight of the total biomass was determined in 100 seedlings of each genotype.

Screen for nadp-mdh *mutants*

The *Arabidopsis nadp-mdh* mutant lines At5g58330::tDNA-50 (Salk_012655) and At5g58330::tDNA-119 (Salk_063444) were obtained from the Arabidopsis Biological Resource Centre (http://www.arabidopsis.org/abrc). Homozygous knockout plants were identified by PCR for T-DNA insertion within the gene region of At5g58330. Genomic DNA was isolated from plant tissues by standard methods. The sequence information for the gene- and T-DNA-specific primers was taken from the Salk Institute (http://signal.salk.edu). The positions of the T-DNA insertion were confirmed by sequencing the PCR products.

Extraction of total RNA and northern blot analysis

For northern blot analysis, total RNA was isolated from frozen leaf material by using the Purescript RNA-extraction kit (Gentra Systems, Minneapolis, MN, USA). For RNA gel-blot hybridization, 10 µg of total RNA were denatured and separated on a 1.0% (w/v) agarose–2.5% (v/v) formaldehyde gel, transferred, and UV-cross-linked to a nylon membrane (Hybond-N, Amersham Biosciences, UK). Pre-hybridization and hybridization were performed at 65 °C in Church buffer medium [0.25 M sodium phosphate buffer, pH 7.2, 1 mM EDTA, 7% (w/v) SDS, and 1% bovine serum albumin (BSA)]. Hybridization was performed with an [α-^{32}P]dCTP-labelled NADP-MDH cDNA-specific probe (Ready-To-Go DNA-labelling beads, Amersham Biosciences, UK). Membranes were washed twice for 15 min at 65 °C in washing buffer [40 mM sodium phosphate buffer, pH 7.2, 1 mM EDTA, 0.5% (w/v) SDS, and 0.5% (w/v) BSA], then for 10 min at room temperature in washing buffer containing 1% (w/v) SDS. Finally, membranes were exposed to a Phosphor-Imager (GE Healthcare, Freiburg, Germany).

RT-PCR analysis

Non-competitive reverse transcription-PCR (RT-PCR) was performed essentially as described by Ahn (2002). cDNA was synthesized from 5 µg of total RNA using oligo(dT) as primer according to the manufacturer's instructions (Fermentas RevertAid™ First Strand cDNA Synthesis Kit, Fermentas GmbH, St. Leon-Rot, Germany). For a 25 µl PCR, 1 µl of cDNA was used as template. The PCR settings were: first cycle at 95 °C for 5 min, then for the optimized number of cycles for each gene product 1 min at 95 °C, 1 min at 47–67 °C, and 1 min at 72°C, and a final extension at 72 °C for 5 min. Oligonucleotides that were used for the detection of the transcripts are listed in Supplementary Table S1 available at *JXB* online. The intensity of each band after electrophoresis was determined with the Quantity One software (BioRad, Munich, Germany).

Microarray analysis

Arabidopsis thaliana 24k oligonucleotide arrays (MWG Biotech; http://www.mwg-biotech.com; ArrayExpress database accession no. A-ATMX-2; http://www.ebi.ac.uk/arrayexpress) were used to study changes in nuclear gene expression. Leaf samples from the WT and *nadp-mdh* knockout plants grown under standard conditions and treated for 7 h with HL (750 µmol quanta m^{-2} s^{-1}) were collected. Following total RNA isolation (Piippo *et al.*, 2006), cDNA synthesis, sample labelling, array hybridization and scanning, as well as spot intensity quantification were performed as in Kangasjärvi *et al.* (2008). The expression data were normalized and analysed by using the tool R/BioConductor limma (Smyth *et al.*, 2003).

Western blot analysis and immunodecoration

Equal amounts of soluble protein (50 µg per lane) were loaded on 12% discontinuous SDS–polyacrylamide gels using a vertical minigel system (Mini-Protean II, BioRad). The gel was blotted onto a nitrocellulose membrane. Immunodecoration was performed essentially as described in Graeve *et al.* (1994). For the detection, polyclonal antisera against NADP-MDH from pea leaves (1:3000), against the 2-Cys Prx BAS1 from barley (to detect 2-Cys PrxA and B; Baier and Dietz, 1997) (1:5000), against the chloroplast-localized NADPH-thioredoxin reductase C (NTRC; Pérez-Ruiz *et al.* 2006) (1:2000), and against the P-protein of glycine decarboxylase (GDC) (1:3000; Hermann Bauwe, Rostock University) were used. For the detection of the second antibody linked to horseradish peroxidase (1:20 000), luminol was used as the substrate as recommended by the supplier (GE Healthcare).

The steady-state levels of the ascorbate peroxidase isoforms tAPX, sAPX, pAPX, and the cytosolic APXs (Asada 1999; Chew *et al.* 2003; Narendra *et al.*, 2006) were analyzed using the anti-APX antibody from Agrisera (http://www.agrisera.com/en/artiklar/apx-ascorbate-peroxidase-.html) as described in Kangasjärvi *et al.* (2008) using 10 µg of total leaf protein and immunodetection with Arabidopsis anti-APX antibody (Kangasjärvi *et al.*, 2008) using a Phototope™-Star Detection Kit (New England Biolabs, Beverly, MA, USA; http://www.neb.com/).

Enzyme measurements in crude extracts

Leaves were cut from the plant, immediately transferred and pulverized in liquid nitrogen, and stored until use at –80 °C. For extraction, buffers as required for the various assays were added to aliquot portions of the powder. The total activity of NADP-MDH was determined after exhaustive reduction with reduced dithiothreitol (DTT) and corrected for unspecific NAD-MDH activity as described by Scheibe and Stitt (1988). The total capacities of catalase and APX were determined in extracts as in Del Longo *et al.* (1993). The enzyme extractions and measurements of the activities of NADP-dependent glyceraldehyde-3-P dehydrogenase (NADP-GAPDH) were performed as in Baalmann *et al.* (1995), of non-phosphorylating GAPDH (NP-GAPDH) as in Rius *et al.* (2006), and of glycerol-3-P dehydrogenase (G3PDH) as in Shen *et al.* (2006).

Chlorophyll (Chl) fluorescence measurements

A portable photosynthesis system LI-6400XT (LI-COR Biosciences, Lincoln, NE, USA) was used to measure leaf Chl fluorescence in 800 µmol quanta m^{-2} s^{-1} actinic light (Table 2), while for measurements in 50 µmol quanta m^{-2} s^{-1} the closed FluorCam FC 800-C (Photon Systems Instruments, Brno, Czech Republic) was used. The intensity of the saturating pulse was 5000 µmol quanta m^{-2} s^{-1} with a duration of 800 ms. The dark adaption time was 20 min. Maximum quantum yield in dark-adapted leaves (F_v/F_m), the quantum yield of photosystem II [PSII; (ΦII)] and the quenching coefficients photochemical quenching (qP) and non-photochemical quenching (NPQ) were calculated according to Schreiber *et al.* (1986), Walker (1988), and Genty *et al.* (1989).

Photosynthetic and respiratory performance of mesophyll protoplasts

Mesophyll protoplasts were isolated from leaves of 11- to 12-week-old WT and *nadp-mdh* plants that had been maintained under the growth conditions as described above. Leaf sections without a midrib were freed of the lower epidermis mechanically with a forceps and subjected to enzymatic digestion with 1% (w/v) Cellulase Onozuka R-10 and 0.4% (w/v) Macerozyme R-10 (Yakult Pharmaceutical Industry, Tokyo, Japan) as described (Riazunnisa *et al.*, 2007).

Rates of respiratory O_2 uptake in the dark and of photosynthetic O_2 evolution in the light by mesophyll protoplasts of WT and *nadp-mdh* mutants were monitored at 25 °C using a Clark-type O_2 electrode (Model DW2, Hansatech Ltd, King's Lynn, UK). The reaction medium for both photosynthesis and respiration determination was 1 ml containing 0.65 M sorbitol, 1 mM $CaCl_2$, 1 mM $MgCl_2$, and 1 mM $NaHCO_3$ in 10 mM HEPES-KOH, pH 7.5, and protoplasts equivalent to 10 µg Chl (Riazunnisa *et al.*, 2007). Illumination with 750 µmol quanta m^{-2} s^{-1} was provided by a 35 mm slide projector (halogen lamp: Xenophot 24 V:150 W). The inhibitors [SHAM, salicylhydroxamic acid (SHAM), glycine hydroxamate (GHA), and aminoacetonitrile (AAN), all from Sigma-Aldrich Co., St Louis, MO, USA] were added to the reaction medium containing mesophyll protoplasts to obtain the required final concentration, and the protoplasts were pre-incubated in darkness at 25 °C for 5 min before switching on the light. The normal level of O_2 in air-equilibrated reaction medium was 410 nmol ml^{-1}. The reaction medium in the O_2 electrode chamber was bubbled with N_2, resulting in a marked decrease of O_2 to 85 nmol ml^{-1}.

Metabolite analysis

Starch content in leaves was determined according to Batz *et al.* (1995). Malate was determined enzymatically with glutamate-oxaloacetate transaminase (GOT; Sigma-Aldrich Co.) in a coupling reaction as described in a protocol of R-Biopharm GmbH (Darmstadt, Germany). Specifically, 100 mg of *Arabidopsis* leaves were frozen in N_2, ground to powder, resuspended in 1 ml of H_2O, and incubated at 95 °C for 8 min. The supernatant was used for the measurement in buffer containing 100 mM glycylglycine, 100 mM glutamate, 1 mM NAD^+, and GOT (1 U ml^{-1}). The reaction was started by adding 1 U ml^{-1} NAD-MDH (Sigma-Aldrich Co.). For proline determination, *Arabidopsis* leaves (500 mg) were frozen in N_2, ground to powder, and 0.5 ml of 3% sulphosalicylic acid was added. After mixing and centrifugation, 0.5 ml of the supernatant was transferred to a new reaction tube, and proline concentrations were measured colorimetrically using the ninhydrin method (Bates *et al.*, 1973). Global metabolite analysis was performed by gas chromatography–mass spectrometry (GC-MS) as described by Lisec *et al.* (2006).

Glutathione determination

The amounts of reduced and oxidized glutathione (GSH and GSSG, respectively) were determined using the Total Glutathione Detection Kit (Enzo Life Sciences, Lörrach, Germany). For each genotype and treatment, *Arabidopsis* leaves from five plants were frozen in N_2 and then ground to powder, and 50 mg of the tissue was used to prepare the extract. For this, 1 ml of ice-cold 5% metaphosphoric acid was added to the powder and vortexed for 30 s. After centrifugation, 50 µl aliquots of supernatant each were used for total glutathione and oxidized glutathione, respectively. For the latter, samples were incubated with 2-vinylpyridine at room temperature for 1 h prior to the assay. The absorbance was recorded at 405 nm using a plate reader (SPECTRAmax Plus 348, Molecular Devices, Sunnyvale, CA, USA) at 1 min intervals over

a 10 min period. For analysis of the data, the software SoftMax Pro 5.3 (Molecular Devices) was used.

Reactive oxygen species (ROS) determinations

H_2O_2 was quantified in leaf extracts prepared immediately after exposure to HL for 5 h, as described by Liu *et al.* (2010). The extract was diluted accordingly and then used for H_2O_2 determination with an Amplex Red Hydrogen Peroxide/Peroxidase Assay Kit (Molecular Probes, Eugene, OR, USA). The values were obtained from three samples, each from two plants, and the standard error was calculated. The data were analysed by analysis of variance (ANOVA), and means were compared using a Student's *t*-test.

Chl and protein determination

To determine leaf Chl *a* and *b* contents, extraction, photometric measurements, and calculation were performed as described in Sims and Gamon (2002). The protein content in the soluble leaf extracts was estimated according to Bradford (1976), with BSA as the standard.

Results

Verification of NADP-MDH *gene knockout in two independent lines of* A. thaliana

Two independent *nadp-mdh*-T-DNA insertion lines were identified in *Arabidopsis*. The lines *At5g58330::*tDNA-50 and *At5g58330::*tDNA-119 harbour a T-DNA insertion at positions 54 200 and 55 324, respectively, of chromosome 5 (Fig. 1A). The combination of the *NADP-MDH*-specific primers 119LP and 119RP for line 119 allowed for amplification of the expected PCR product (1028 bp) on genomic DNA from the WT, but not on DNA from homozygous *nadp-mdh* knockout plants from line 119 (Supplementary Fig. S1A at *JXB* online). For line 50, the gene-specific primers 121 and 84 were used and the corresponding PCR product had a size of 1320 bp (Supplementary Fig. S1B). PCR products were amplified in reactions containing the T-DNA left border primer LBa1 and one gene-specific primer on DNA from both homozygous *nadp-mdh* mutant lines, but not on DNA from WT plants (Supplementary Fig. S1A, B). The PCR result and the sequencing of the PCR products confirmed that in both cases homozygous T-DNA plants had been obtained.

Both homozygous lines lacked the *NADP-MDH* transcript as indicated by northern blot analysis (Supplementary Fig. S2A at *JXB* online) and RT-PCR (data not shown), and were devoid of the NADP-MDH protein as demonstrated by western blot analysis (Supplementary Fig. S2B). NADP-MDH activity, when corrected for the unspecific activity with NADPH oxidation derived from NAD-MDH isoforms (Scheibe and Stitt, 1988), was also completely absent (data not shown). The results validated both insertion lines as full *nadp-mdh* knockout lines. Given that the two insertion lines exhibited identical phenotypes, further work was concentrated on line 50, but selected results were also confirmed using line 119.

Phenotypic appearance of nadp-mdh *plants*

The phenotype of *nadp-mdh* plants under standard growth conditions (GL: 50 µmol quanta m^{-2} s^{-1}, short-day) on soil was indistinguishable from that of the WT (Fig. 1B). Likewise, Chl *a*, Chl *b*, and protein contents as well as fresh weight and water content were not significantly altered in the *nadp-mdh* plants (Table 1).

Cultivation of WT plants under stress conditions such as HL, low temperature, or fluctuating light stimulates expression of *NADP-MDH*, indicating the requirement for an increased capacity of the malate valve (Becker *et al.*, 2006). In this study, *nadp-mdh* plants treated with either HL or low temperature also revealed an unaltered phenotype compared with the WT. The GL-acclimated *nadp-mdh* mutant plants that were transferred to HL for 1 week (Fig. 1C), as well as the plants that were cultivated under HL for the complete growth period (Fig. 1D, E), developed a WT-like phenotype. Even under the more variable climatic conditions of a greenhouse, the potted mutants developed like the WT (data not shown).

HL effects on ROS formation and antioxidative systems

Accumulation of NADPH in the *nadp-mdh* plants could stimulate the Mehler reaction and concomitantly increase ROS formation during HL conditions. In the mutants, a decreased level of ROS was apparent compared with the WT, in HL as well as GL (Fig. 2A). The reduced and oxidized glutathione increased in both the WT and mutants upon exposure to HL, but the redox state was unaffected by the lack of chloroplast NADP-MDH (Fig. 2B). The protein levels, transcript amounts, and activities of selected Beck–Halliwell–Asada pathway enzymes were examined in WT and *nadp-mdh* mutant plants. No difference could be detected in either protein levels of the various APX isoforms (Fig. 2D) or the total APX activity (Fig. 2E). Semi-quantitative RT-PCR analysis revealed a strong up-regulation of sAPX transcript and a slight up-regulation of tAPX, dehydroascorbate reductase (DHAR), monodehydroascorbate reductase (MDAR), and glutathione reductase (GR) after HL treatment (Fig. 2C; Supplementary Fig. S3 at *JXB* online).

To address the ascorbate-independent water–water cycle, the expression of NTRC and the various chloroplast Prx isoforms in leaves of WT and *nadp-mdh* plants was analysed, after 7 h HL. NTRC transcript and protein levels were increased in the *nadp-mdh* plants after 7 h of HL (Fig. 3A, B), as were the transcript levels of chloroplast 2-Cys Prx isoforms PrxIIE and PrxQ (Fig. 3A), whereby the increase of the PrxA/B and PrxIIE transcripts was significant. In contrast to transcript regulation, the amount of 2-Cys PrxA/B protein (named BAS1; Baier and Dietz, 1997) was unchanged in both genotypes after HL treatment (Fig. 3C). Transcriptome profiling revealed an increase in some transcripts, among the most prominent being a C3HC4 zinc finger RING-type protein (At4g26400), a WRKY-family (At4g31550), and a MYB-related (At4g01060) transcription factor (Supplementary Fig. S3 at *JXB* online). These transcription factors are also found to be increased in *EXECUTER* mutants where signalling from the chloroplast to the nucleus is affected (Lee *et al.*, 2007).

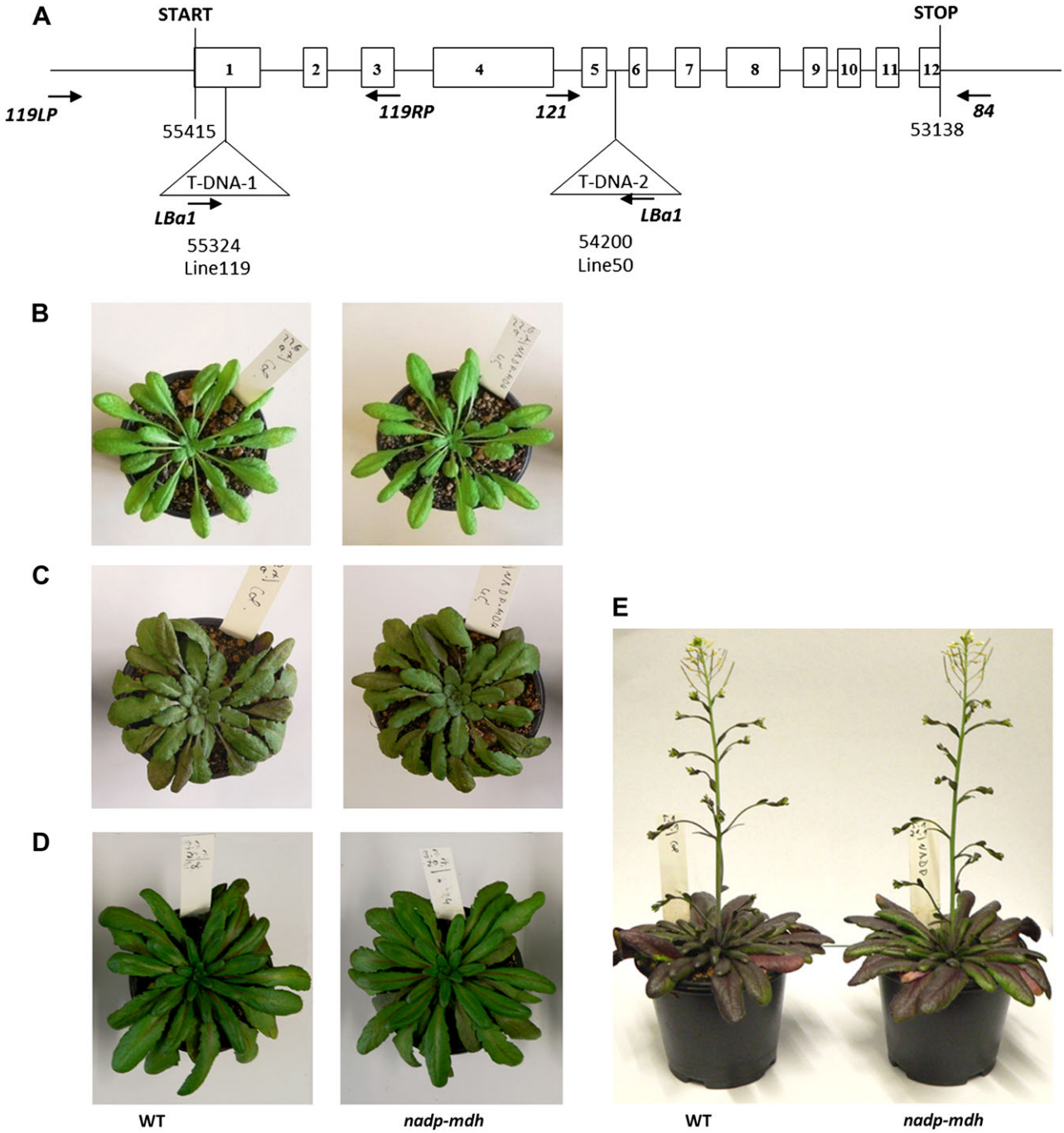

Fig. 1. Genome insertion sites and phenotype of the two independent homozygous *nadp-mdh* (At5g58330) mutants. (A) Gene structure of the two individual *At*NADP-MDH-T-DNA insertion lines Salk 012655 (line 50) and Salk 063444 (line 119). The insertion in line 50 is localized in the fifth intron, whereas in line 119 the insertion is localized in the first exon. The primers used for PCR analysis are marked as arrows. (B) Phenotype of plants of line 50 grown for 8 weeks under standard growth conditions at 50 μmol quanta m^{-2} s^{-1} under a short-day photoperiod. (C) Plants were grown for 8 weeks under standard growth conditions (50 μmol quanta m^{-2} s^{-1}) and then transferred to HL (750 μmol quanta m^{-2} s^{-1}) for 7 d. (D and E) Plants were cultivated under HL (750 μmol quanta m^{-2} s^{-1}) during their entire growth period.

Photosynthetic performance and photorespiratory components in WT and nadp-mdh *plants under HL conditions*

Photosynthetic CO_2 assimilation rates as a function of light intensities were quite similar in leaves of *nadp-mdh* and WT plants (data not shown). Chl fluorescence was used to monitor the redox state of PSII in WT and *nadp-mdh* plants after growth in moderate light (GL), after growth in HL (750 μmol quanta m^{-2} s^{-1}) for long-term acclimation, and during a HL treatment in the measurement (~20–30 min) after growth in GL for short-term acclimation. Under all conditions, no significant differences in the efficiency of

Table 1. *Leaf characteristics of WT and* nadp-mdh Arabidopsis *plants*

Arabidopsis plants were grown for 11 weeks under GL (50 μmol quanta m^{-2} s^{-1}), then the leaves were analyzed.

	WT	*nadp-mdh*
Specific fresh weight (mg cm^{-2})	18.09±1.14	17.93±1.10
Water content (%)	92.49±0.31	92.11±0.41
Chl *a* (μg cm^{-2})	5.21±1.34	5.56±1.66
Chl *b* (μg cm^{-2})	2.10±0.55	2.2±0.59
Protein (μg cm^{-2})	157.30±6.89	157.18±15.20
Starch as glucose units (μmol mg^{-1} Chl)	27.35±0.37[a]	27.49±2.20[a]

[a] After 1 d of HL treatment.

dark-adapted PSII (F_v/F_m), qP, NPQ, and flux through PSII (ΦII) were apparent in the mutants as compared with the WT (Table 2). Also P700 absorption in leaves under GL as well as HL conditions was not significantly altered between the WT and mutant (data not shown). These observations indicate that neither a higher reduction state of the primary electron acceptor Q_A in PSII, nor a higher rate of cyclic electron transport, nor photoinhibition occurred in the mutants under HL.

Excess photosynthetic reductant could be consumed during the reactions of photorespiration, depending on the levels of CO_2 and O_2. Gas exchange experiments on leaves indicated a possibly increased photorespiratory component in *nadp-mdh* mutants (data not shown). Therefore, an effect of HL on photorespiratory activity was further investigated in protoplasts of *nadp-mdh* knockout and WT plants. The photosynthetic rates of mesophyll protoplasts from WT leaves were not significantly changed at low O_2 compared with ambient O_2 when assayed at 1 mM bicarbonate in the assay medium, while in the mutants photosynthesis was strongly inhibited at low O_2 compared with normal air (Fig. 4A). Further, the transcript levels of GDC1 and GDC2 (P-protein) were higher in the mutant than in the WT after 7 h of HL treatment (Fig. 4B), while the immunoblot indicated only a slight increase or no change in P-protein in the mutant (Fig. 4C). Other activities related to photorespiration, namely catalase and hydroxypyruvate reductase, were not affected in whole leaf extracts following 7 h of HL treatment, either in the WT or in the mutant plants (data not shown).

Effect of lacking a malate valve on mitochondrial activities and metabolite levels upon HL treatment

The *AOX1A* transcript level increased to a similar extent in both genotypes when transferred from GL to HL (Fig. 5B). However, the inhibitory effect of SHAM on photosynthesis of protoplasts was more pronounced in mutants than in the WT (Fig. 5A), suggesting an important role for mitochondrial AOX in compensating the loss of chloroplast NADPH-MDH. This was true both at low O_2 and in normal air (Fig. 5A).

Metabolite profiling using GC-MS revealed differences in relative metabolite contents between WT and *nadp-mdh* plants under GL (the full data set is presented in Supplementary Table S2 at *JXB* online). However, the relative differences in metabolite contents were pronounced following a 7 h HL treatment. The most significant metabolic differences between the WT and mutants are presented in Fig. 6 and include increases in aspartate, proline (>2-fold), and succinate, along with decreases in glutamine, 5-oxoproline, malate, and, tentatively, ascorbate (Fig. 6). The levels of sucrose and starch were unaltered between mutant and WT plants (Fig. 6, Table 1). Starch levels decreased to very low levels during the following dark phase in both genotypes (Table 1).

The decreased malate level in the mutants after 7 h of HL was confirmed by an enzymatic determination yielding 18.0 μmol g^{-1} fresh weight in the WT and 15.0 μmol g^{-1} fresh weight in the mutant (Fig. 7A). Intriguingly, there was a 2.1-fold increase in proline in the mutants following the exposure to HL, while it increased only 1.5-fold in the WT (Fig. 7B).

Enzyme activities of alternative shuttle systems

Indirect transfer of reducing equivalents from the chloroplast to the cytosol and subsequently into mitochondria might alternatively be mediated by oxidoreductases other than MDH, in conjunction with appropriate transporters. The enzyme activities of NADP-GAPDH of the Calvin cycle, cytosolic NP-GAPDH, and mitochondrial NAD-dependent G3PDH, thought to be involved in a mitochondrial shuttle for reducing equivalents (Shen *et al.*, 2006) were therefore determined. The activity of only NADP-GAPDH was increased in the *nadp-mdh* mutants (Table 3).

Effect of lacking NADP-MDH on early seedling growth

Although there was no difference in biomass between the WT and mutants at the mature stage (Fig. 1), in the early stages of growth the mutants had a clear advantage, either when directly cultivated as single plantlets on soil, or on agar under sterile conditions with minimal medium containing 1.8 mM nitrate (Fig. 8). The mutant seedlings had a significantly increased biomass after either 4 weeks of growth on agar or 5 weeks of growth on soil, when grown under 150 μmol quanta m^{-2} s^{-1}.

Discussion

Flexibility in redox metabolism prevents phenotypic alterations in nadp-mdh *plants*

Experimental evidence and theoretical considerations suggest that the malate valve can counteract over-reduction of the photosynthetic electron transport chain (Scheibe, 2004). Therefore, it was surprising to observe the WT-like performance of *nadp-mdh* plants even when cultivated under HL conditions, for example with respect to photosynthetic performance and development (Table 1; Fig. 1). Obviously, these mutants do not use excess reducing equivalents in the Calvin cycle for CO_2 fixation and for biomass production as

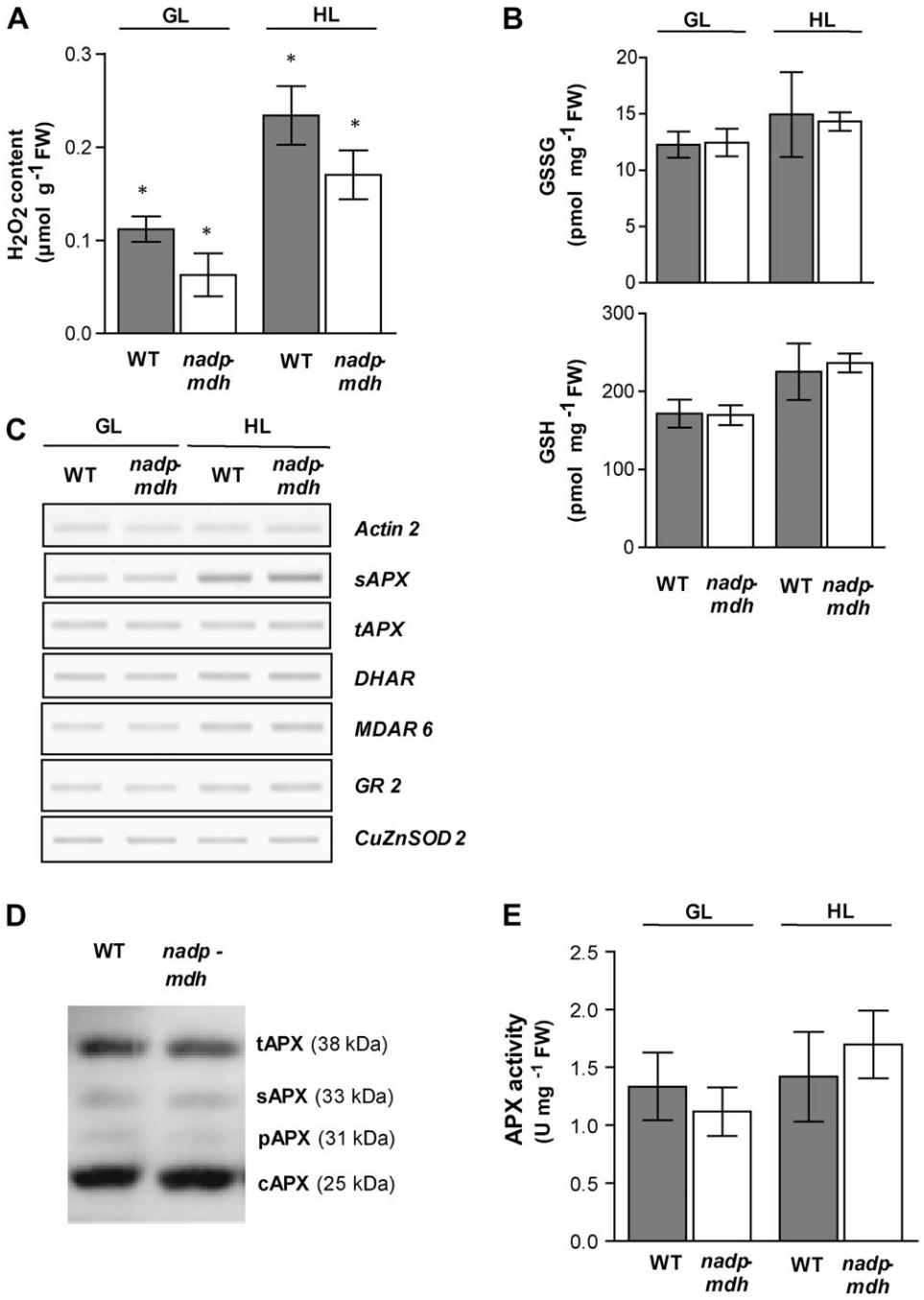

Fig. 2. Quantification of ROS and the Beck–Halliwell–Asada antioxidant system. (A) Quantitation of ROS in extracts using Amplex Red. Asterisks indicate that the differences ($P < 0.05$) between the WT and *nadp-mdh* mutants are statistically significant as determined by the *t*-test. (B) Contents of GSH and GSSG in WT and *nadp-mdh* plants. Values are presented as the mean ±SD of six individual determinations per genotype. (C) Semi-quantitative RT-PCR for transcript analysis of Beck–Halliwell–Asada pathway enzymes. RNA was isolated from WT and mutant plants maintained in GL or transferred to HL for 7 h, transcribed in cDNA, and amplified by PCR at the linear amplification rate using the primers listed in Supplementary Table S1 at *JXB* online. The following transcripts were analysed: sAPX (At4g08390; chloroplast/mitochondria), tAPX (At1g77490; chloroplast), stromal DHAR (At5g16710; chloroplast), MDAR 6 (At1g63940; chloroplast/mitochondria), GR 2 (At3g54660; chloroplast/mitochondria), and CuZnSOD 2 (At2g28190; chloroplast/apoplast). The result is representative for two independent experiments. (D) Western blot of an SDS–gel with crude extracts from leaves of WT and *nadp-mdh* plants, and immunodecoration with antiserum against APX isoforms. (E) Total APX activity

evidenced by the identical CO_2 assimilation rates of leaves, similar photosynthesis rates in isolated protoplasts (Fig. 4A), and unaltered levels of the photosynthetic products, sucrose and starch (Fig. 6, Table 1). An inhibitory effect on the growth rate was detected in antisense tobacco plants expressing <10% of WT amounts of NADP-MDH when grown under natural light conditions in a greenhouse (Faske *et al.*, 1997). Overexpression of NADP-MDH

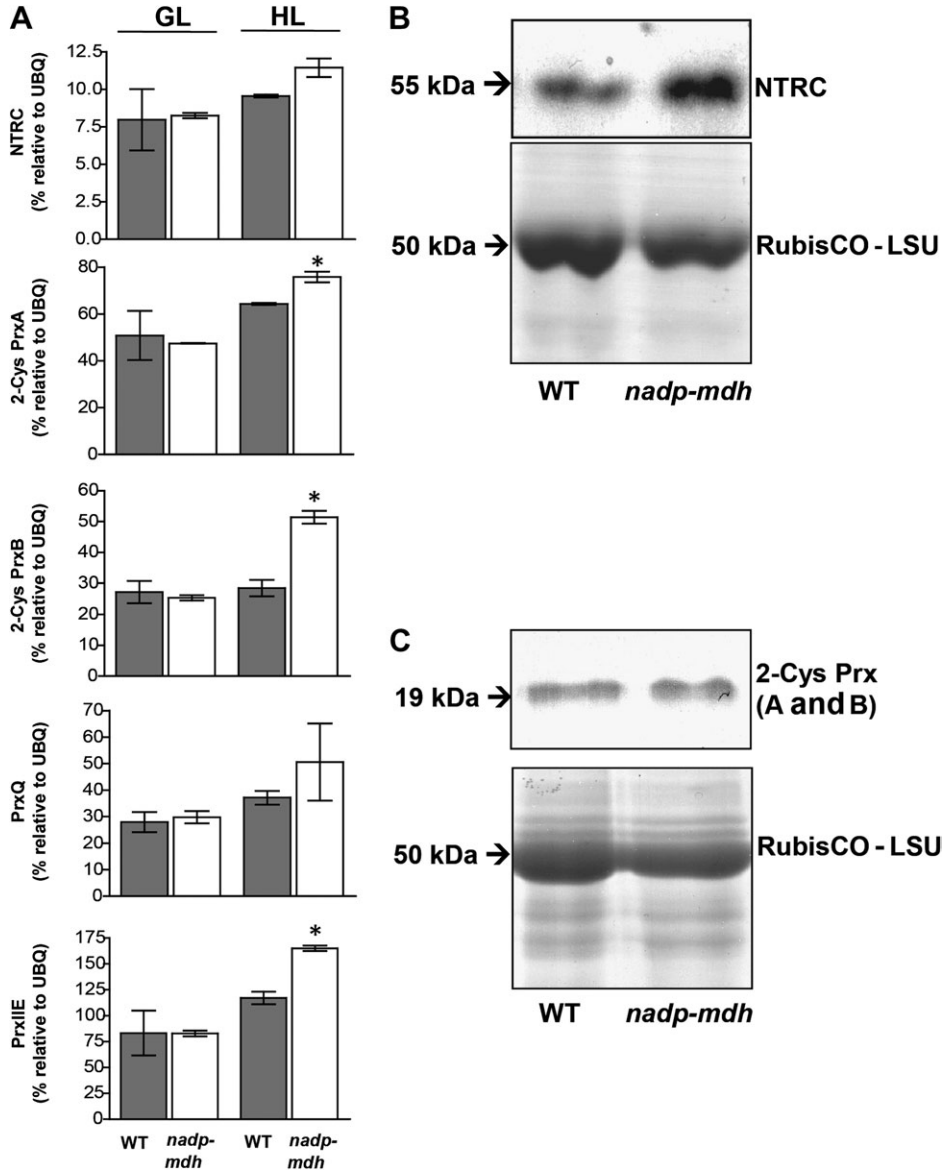

Fig. 3. Transcript and protein levels of the NTRC and chloroplast Prx system. (A) Densitometric analysis of RT-PCR for NTRC, 2-Cys PrxA/B, PrxQ, and PrxIIE in leaves of WT and *nadp-mdh* knockout plants after 7 h of HL treatment. Ubiquitin (UBQ) was used as the reference transcript. (B and C) Protein amounts of NTRC and 2-Cys Prx. Western blot and immunodetection using antiserum against NTRC and 2-Cys Prx were performed with extracts from WT and *nadp-mdh* knockout plants after 7 h of HL treatment. In the lower part, the Coomassie-stained band of the RubisCO large subunit (LSU) is shown as a loading control. Asterisks indicate that the differences ($P < 0.05$) between WT and *nadp-mdh* mutants are statistically significant as determined by the *t*-test.

Table 2. *Photosynthetic parameters of WT and* nadp-mdh Arabidopsis *plants under GL and HL conditions*

Experiment[a]	50/50		750/50		50/750	
	WT	***nadp-mdh***	**WT**	***nadp-mdh***	**WT**	***nadp-mdh***
F_v/F_v	0.84±0.00	0.84±0.00	0.75±0.03	0.74±0.03	0.81±0.01	0.81±0.01
qP	0.80±0.04	0.82±0.01	0.86±0.04	0.88±0.02	0.32±0.02	0.31±0.03
NPQ	0.26±0.04	0.19±0.04	0.23±0.05	0.27±0.14	1.97±0.14	1.84±0.13
ΦII	0.64±0.01	0.66±0.01	0.61±0.01	0.62±0.04	0.17±0.02	0.16±0.01

[a] Each set of data in the three experiments was generated with a different combination of light intensities during pre-treatment and measurement for WT and mutant plants, e.g. 50/50: pre-treatment of the plants at 50 μmol quanta m^{-2} s^{-1}, measurement at 50 μmol quanta m^{-2} s^{-1}.

stimulated tobacco plant development until the pot size became limiting (Faske *et al.*, 1997).

In this study, the photosynthetic electron transport was also broadly unaffected by altered NADPH+H^+ oxidation

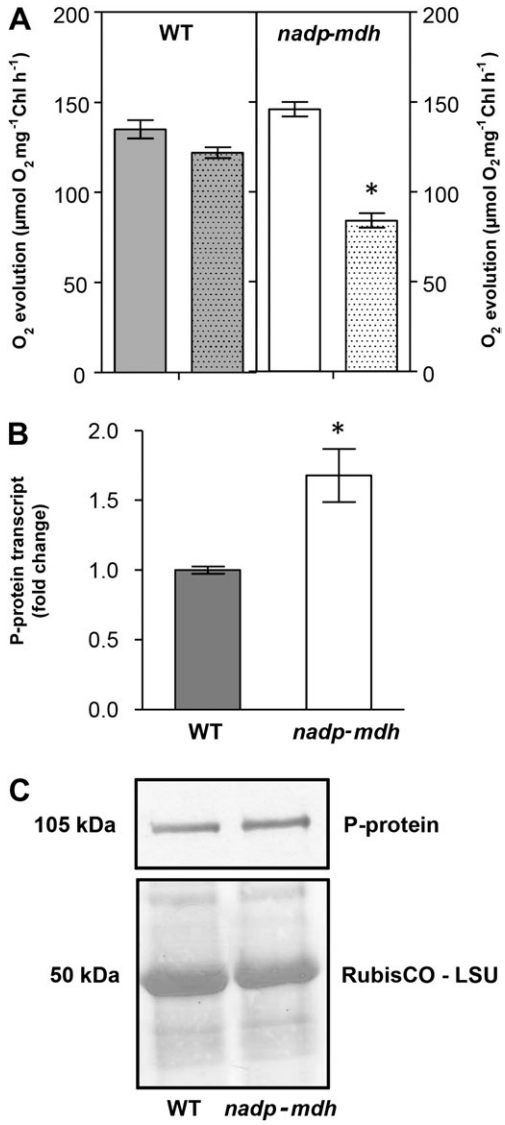

Fig. 4. Effect of inhibition of photorespiration on photosynthesis in protoplasts. (A) Rates of photosynthetic O_2 evolution by protoplasts from WT (grey bars) and *nadp-mdh* knockout mutants (white bars) at an optimal bicarbonate concentration (1 mM) under either normal O_2 (~410 nmol O_2 ml^{-1}) (empty bars) or low O_2 (~85 nmol O_2 ml^{-1}) (dotted bars). (B) Densitometric analysis of RT-PCR for GDC1/2 (P-protein) expression in leaves of WT and *nadp-mdh* plants after 7 h of HL treatment. Ubiquitin (UBQ) transcript was used for normalization. (C) Western blot and immunodetection using antiserum against the P-protein of GDC were performed with extracts from WT and *nadp-mdh* knockout plants after 7 h of HL treatment. The lower part depicts a Coomassie-stained gel showing the intensity of the band for RubisCO large subunit (LSU). Data represent mean values (±SE) from at least three independent experiments. Asterisks indicate that the differences ($P < 0.05$) between normal and low oxygen (in A) and also between WT and *nadp-mdh* (in B) are statistically significant as determined by the *t*-test.

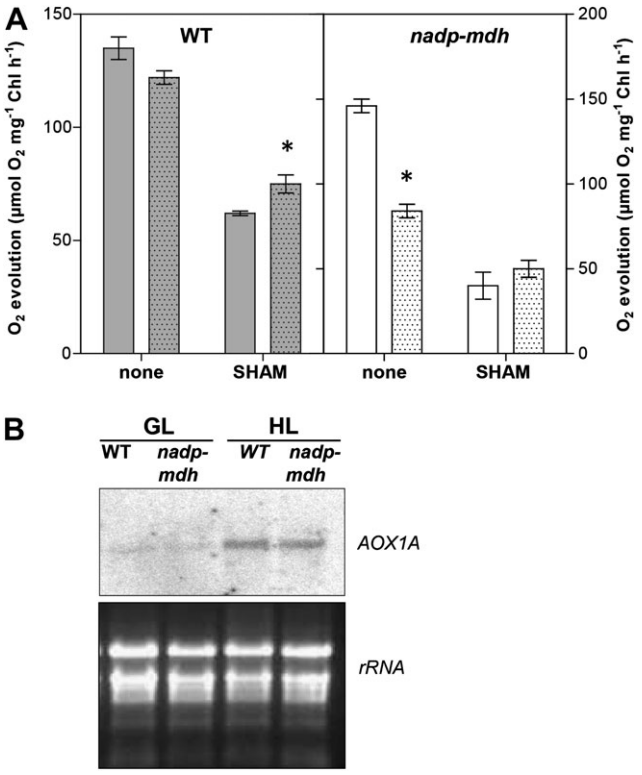

Fig. 5. Components of the mitochondrial electron transport. (A) Rates of photosynthetic O_2 evolution by protoplasts from WT (grey bars) and *nadp-mdh* knockout mutants (white bars) at an optimal bicarbonate concentration (1 mM) under either normal O_2 (~410 nmol O_2 ml^{-1}) (empty bars) or low O_2 (~85 nmol O_2 ml^{-1}) (dotted bars) without inhibitors and with SHAM (600 μM). (B) Effects of HL treatment on *AOX1A* expression. Northern blot analysis of WT and *nadp-mdh* knockout plants after 7 h under GL (50 μmol quanta m^{-2} s^{-1}) and after 7 h under HL (750 μmol quanta m^{-2} s^{-1}), respectively. Total RNA was extracted from leaves. Ethidium bromide staining confirmed equal RNA loading. The blot was hybridized with an *AOX1A*-specific probe. Asterisks indicate that the differences ($P < 0.05$) between normal and low oxygen are statistically significant as determined by the *t*-test.

capacity as an electron acceptor in *nadp-mdh* plants (Table 2). Likewise, potato plants expressing minimal amounts of NADP-MDH (≤10% of the WT) are able to adjust photosynthesis and CO_2 assimilation for unaffected performance, most probably by employing various energy-dissipating cycles at PSI and PSII (Laisk *et al.*, 2007). Since there is no evidence for over-reduction at PSII even in the *nadp-mdh A. thaliana* plants under HL conditions (Table 2), it is expected that these mutants use compensatory strategies to protect themselves from excess reductant in chloroplasts and subsequent oxidative stress.

A set of diverse mechanisms can help to avoid development of oxidative damage (Noctor and Foyer, 1998; Niyogi, 2000; Scheibe *et al.*, 2005; Hanke *et al.*, 2009; Scheibe and Dietz, 2011). The analysis of the mutants, lacking *nadp-mdh*, revealed a novel combination of different mechanisms to cope with excess reducing equivalents as discussed below: (i) a stimulated NTRC/2-Cys Prx system; (ii) adjustments in photorespiratory metabolism; and (iii) possibly, proline biosynthesis.

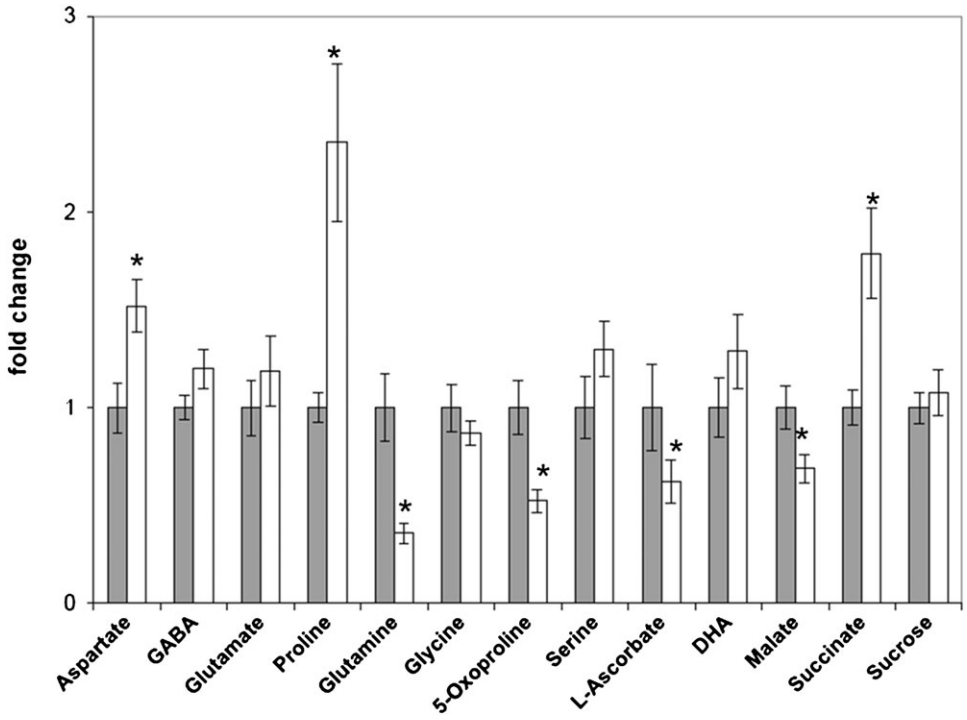

Fig. 6. Normalized metabolite contents of WT and *nadph-mdh* plants after 7 h of HL treatment. Relative metabolite contents were determined in leaf discs of 11-week-old WT plants (grey bars) and *nadp-mdh* mutants (white bars). Data were normalized with respect to the mean response calculated for the WT. Values are presented as the mean ±SE of n=6 per genotype. An asterisk indicates values that were determined by the t-test to be significantly different ($P < 0.05$) from the WT.

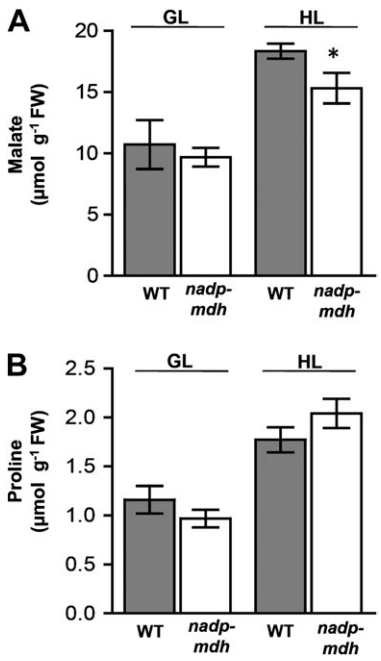

Fig. 7. Malate and proline content. (A) Malate content in leaves of WT (grey bars) and *nadp-mdh* mutants (white bars) under GL and under 7 h HL, respectively. (B) Proline content in WT and *nadp-mdh* mutants after 7 h under GL and under HL, respectively. Asterisks indicate that the differences ($P < 0.05$) between WT and *nadp-mdh* mutants are statistically significant as determined by the t-test.

Table 3. Activities (mU mg^{-1} protein) of oxidoreductases possibly involved in redox shuttles

	WT	*nadp-mdh*
NADP-GAPDH	167.63±17.03	232.06±16.70
NP-GAPDH	24.38±2.29	22.57±1.14
NAD-G3PDH	7.47±1.26	6.38±2.16

ROS production and the importance of the NTRC/Prx-based antioxidative system

One might expect stimulated electron transfer to O_2, and thus increased ROS production and oxidative stress, in plants lacking the malate valve. Glutathione (GSH) and ascorbate are important to protect plants from oxidative damage (Noctor and Foyer, 1998; Mullineaux and Rausch, 2005), through the Beck–Halliwell–Asada pathway (Foyer and Halliwell, 1976) and in the GSH–glutaredoxin-type II Prx pathway (Tripathi *et al.*, 2009). However, there were no marked changes in either glutathione (Fig. 2B) or ascorbate/DHA (Fig. 6). Expression of various enzymes of the Beck–Halliwell–Asada cycle in *nadp-mdh* plants was also unchanged, even in HL (Fig. 2C–E). This suggests that the ROS-scavenging systems, based on the ascorbate/glutathione and Beck–Halliwell–Asada pathway, are unaffected in *nadp-mdh* plants. However, the mutant plants showed increased levels of the NTRC/Prx system.

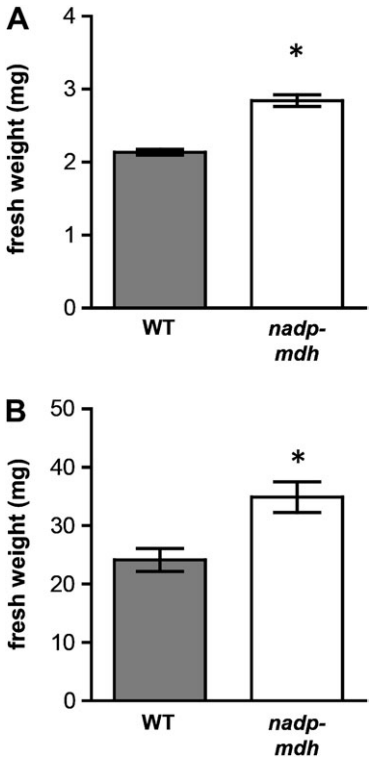

Fig. 8. Seedling growth on agar under sterile conditions and on soil. (A) Sterilized seeds were placed on agar containing 1.8 mM nitrate as an N source, and seedlings were grown for 5 weeks under short-day conditions in sealed Petri dishes. The fresh weight of 100 seedlings of each genotype with standard deviations is given. (B) Seeds were grown in pots with soil, and the fresh weight of the above-ground biomass was determined for 100 seedlings of each genotype at 5 weeks of age. Asterisks indicate that the differences ($P < 0.05$) between WT and *nadp-mdh* mutants are statistically significant as determined by the *t*-test.

Besides the Beck–Halliwell–Asada pathway, the NTRC/Prx system quenches H_2O_2 in the chloroplast (König *et al.*, 2002; Serrato *et al.*, 2004; Pérez-Ruiz *et al.*, 2006) and this peroxide detoxification cycle was named the ascorbate-independent or Prx-dependent water–water cycle (Dietz *et al.*, 2006). Recent studies using knock-down plants show that the NTRC-dependent regeneration of 2-Cys Prx is more important than the thioredoxin-dependent one (Pulido *et al.*, 2010). In *nadp-mdh* mutants under HL, *2-Cys Prx B* and *NTRC* transcripts, as well as NTRC protein increased compared with WT plants (Fig. 3A, B). Data from Spinola *et al.* (2008) indicate that the NTRC system plays a specific role in eliminating ROS in the dark, and this point explains that stress treatment in the dark has more effect on *Arabidopsis ntrc* knockout lines than on WT plants (Pérez-Riuz *et al.*, 2006). In *nadp-mdh* plants too, the Prx-dependent water–water cycle appears to function as an alternative poising system that is increased to use up NADPH when malate cannot be formed (Fig. 9). Transcript profiling gave no additional clues as to which alternative pathways might have been up-regulated (Supplementary Fig. S3 at *JXB* online).

Adjustments in components of photorespiration, mitochondria, and proline biosynthesis may all compensate for the lack of malate valve

Despite being a major source of ROS, photorespiration is crucial for maintaining the redox state in plant cells (Foyer *et al.*, 2009; Bauwe *et al.*, 2010). Therefore, in *nadp-mdh* plants, the photorespiratory pathway may provide an alternative mechanism to transport excess reducing equivalents from the chloroplast to the mitochondrion, facilitating electron transfer to O_2 via the cytochrome *c* oxidase pathway or AOX (Fig. 9). Transcript profiling of mutant plants lacking NTRC had increased transcript levels for photorespiratory genes such as those coding for catalase, P-protein, and hydroxypyruvate reductase, and showed multiple signs of metabolic imbalances (Lepistö *et al.*, 2009). The marked decrease in photosynthesis of protoplasts under low oxygen (Fig. 4A), high expression of GDC (Figs. 4B, C), and a shift in the glycine-to-serine ratio (Fig. 6) suggest altered patterns in photorespiration of *nadp-mdh* mutants.

Inhibition of AOX or lack of the AOX1A isoform in mitochondria of transgenic plants is known to cause over-reduction of the photosynthetic electron transport chain in the light (Padmasreee and Raghavendra, 1999; Yoshida *et al.*, 2007; Strodtkötter *et al.*, 2009). The increase in protein and activity of AOX under HL and drought (Clifton *et al.*, 2006; Giraud *et al.*, 2008) suggest that AOX plays an important role in the consumption of excess reducing equivalents exported from the chloroplasts in light. Although the malate valve-dependent transport was disabled, the increase in *AOX1A* transcript levels in *nadp-mdh* mutants was similar to that in WT plants after HL treatment (Fig. 6C), indicating activation of alternative pathways for NADH re-oxidation in the mitochondria of both the WT and mutants. Interestingly, transgenic tomato plants with decreased mitochondrial NAD-MDH exhibited even enhanced photosynthetic performance (Nunes-Nesi *et al.*, 2005), indicating the redundancy of some of the oxidative processes involved in optimizing photosynthesis. In double mutants expressing neither mitochondrial MDH isoform, photorespiration was increased (Tomaz *et al.*, 2010).

Possible function of proline in nadp-mdh *knockout plants*

The increased proline contents of *nadp-mdh* mutants in HL (Figs 6, 7B) might represent a strategy of the plants to increase stress tolerance, since proline functions as a compatible solute in drought/salt stress (Hare *et al.*, 1999) and stabilizes the redox status of the cell (Bellinger and Larher, 1987; Hare *et al.*, 1999; Szabados and Savouré, 2009). Further experiments are needed to confirm that the accumulation of proline in the *nadp-mdh* mutants under HL can help to consume excess NADPH (Fig. 9).

Early seedling growth

A highly reproducible increase in biomass occurred in the mutant plants during early development when grown on soil, or on agar under sterile conditions with 1.8 mM nitrate

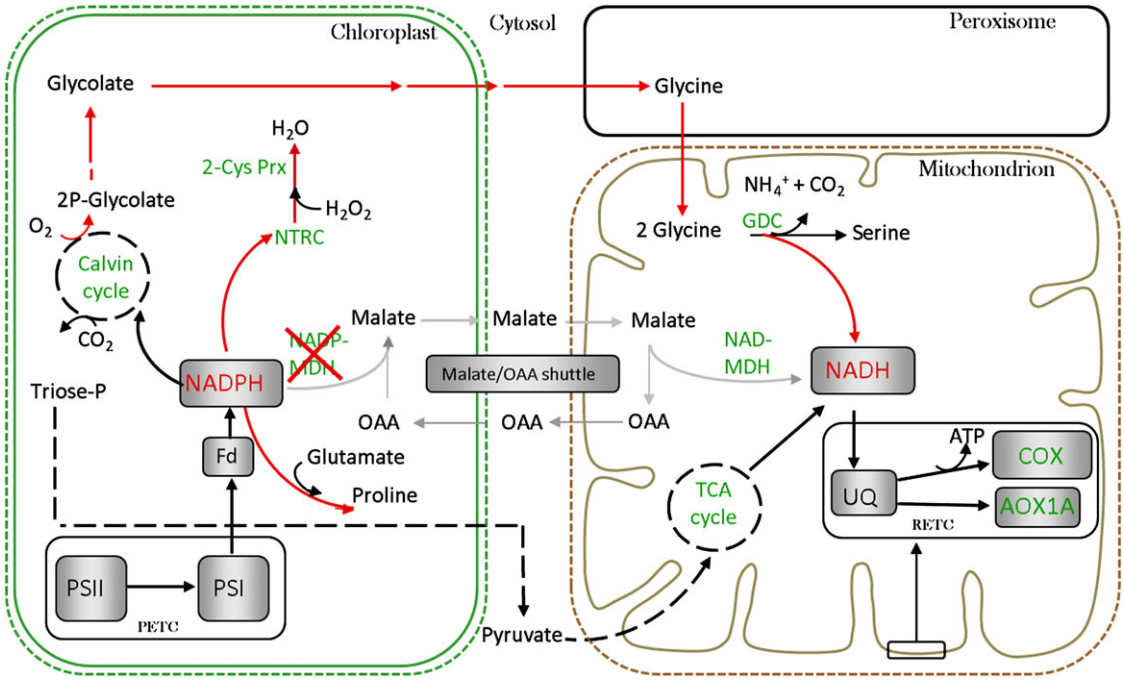

Fig. 9. Overview of compensatory pathways which prevent over-reduction and overenergization of the chloroplast in *nadp-mdh* knockout mutants. The pathways which are stimulated in mutants are all shown by red arrows, normal pathways in black, and suppressed routes in grey. See text for further description.

in minimal medium (Fig. 8). The compensatory responses in the *nadph-mdh* plants seem to become established early to achieve a metabolic pattern and altered redox state which are even beneficial under certain conditions.

Conclusions

The *nadp-mdh* mutants employ a combination of mechanisms to compensate for the lack of the malate valve function under HL conditions. Higher capacity of the NTRC system, along with increased expression of Prxs could facilitate balancing the NADP/NADPH ratio in the chloroplasts and sustain ROS scavenging. Adjustments in photorespiratory components might also reflect the need to dissipate excess reducing equivalents and prevent photoinhibition. Further experiments are required to establish the role of proline as a protective mechanism against oxidative stress in *nadp-mdh* mutants. It is suggested that ROS may act as a 'prime' to trigger changes initially in chloroplasts and then in other compartments of plant cells, resulting in acclimation of *nadp-mdh* plants.

Supplementary data

Supplementary data are available at *JXB* online.

Figure S1. PCR analyses for proof of homozygous T-DNA insertion and *NADP-MDH* gene knockout.

Figure S2. Northern blot (A) and western blot with immunodecoration (B) to document the NADP-MDH (At5g58330) gene knockout in the lines 119 (Salk_063444) and 50 (Salk_012655).

Figure S3. Heatmap showing up- and down-regulated genes in the HL-treated (7 h at 1000 µmol quanta m^{-2} s^{-1}) *nadp-mdh* versus WT plants grown for 5 weeks under 100 µmol quanta m^{-2} s^{-1}, 8/16 h light/dark rhythm. Results from three independent experiments with | log2(expression ratio) | > 1 and *P*-value <0.06 are shown. The analysis was run in R/BioConductor using topTable and heatmap.2 functions.

Table S1. Oligonucleotides used for RT-PCR.

Table S2. Relative metabolite content in WT and *nadp-mdh* mutants grown under low light (GL) and exposed to HL for 7 h.

Acknowledgements

This study was financially supported by the Deutsche Forschungsgemeinschaft to V.L. and R.S. (EM166/1), grants from the Department of Science and Technology-Deutscher Akademischer Austauschdienst (DAAD, to A.S.R. and R.S.), the DAAD-Finland program (to R.S. and E.-M.A.), and by a DFG-Mercator Visiting Professorship to A.S.R. Funds were also received from the Academy of Finland to E.-M.A. (118637, 8133293), P.M. (130075), and S.K. (130595). The authors thank Dr Francisco Javier Cejudo (Sevilla) for the gift of anti-NTRC serum as well as probes for NTRC, and Dr Eevi Rintamäki for the antibody against *Arabidopsis* APXs. We thank Professor Hermann Bauwe (Rostock) for probes and antiserum against GDC (P-protein). We also thank Guiseppe Forlani (Ferrara, Italy) for providing P5C, and Dietmar Funck (Konstanz, Germany) for advice concerning proline metabolic enzyme measurements. Thanks are due to Silke Walter for expert technical assistance. We also thank Heike Wolf-Wibbelmann and Kirsten Jäger for cultivating the plants, and

Heike Schwiderski and Nicolas König for their help with the preparation of the manuscript.

References

Ahn JH. 2002. Noncompetitive RT-PCR. In: Weigel D, Glazebrook J, eds. *Arabidopsis. A laboratory manual*. Cold Spring Harbor, NY: Cold Spring Harbor Laboratory Press, 174–176.

Asada K. 1999. The water–water cycle in chloroplasts: scavenging of active oxygens and dissipation of excess photons. *Annual Review of Plant Physiology and Plant Molecular Biology* **50,** 601–639.

Baalmann E, Backhausen JE, Vetter S, Scheibe R. 1995. Reductive modification and non-reductive activation of purified spinach chloroplast NADP-glyceraldehyde 3-phosphate dehydrogenase. *Archives of Biochemistry and Biophysics* **324,** 201–208.

Baier M, Dietz KJ. 1997. The plant 2-Cys peroxiredoxin BAS1 is a nuclear-encoded chloroplast protein: its expressional regulation, phylogenetic origin, and implications for its specific physiological function in plants. *The Plant Journal* **12,** 179–190.

Bates LS, Waldren RP, Teare ID. 1973. Rapid determination of free proline for water-stress studies. *Plant and Soil* **39,** 205–207.

Batz O, Scheibe R, Neuhaus HE. 1995. Purification of chloroplasts from fruits of green-pepper (*Capsicum annuum* L.) and characterization of starch synthesis. Evidence for a functional hexose-phosphate translocator. *Planta* **196,** 50–57.

Bauwe H, Hagemann M, Fernie AR. 2010. Photorespiration: players, partners and origin. *Trends in Plant Science* **15,** 330–336.

Becker B, Holtgrefe S, Jung S, Wunrau C, Kandlbinder A, Baier M, Dietz K-J, Backhausen JE, Scheibe R. 2006. Influence of the photoperiod on redox regulation and stress responses in *Arabidopsis thaliana* L. (Heynh.) plants under long- and short-day conditions. *Planta* **224,** 380–393.

Bellinger Y, Larher F. 1987. Proline accumulation in higher plants: a redox buffer? *Plant Physiology* **6,** 23–27.

Bradford MM. 1976. Rapid and sensitive method for quantitation of microgram quantities of protein utilizing the principle of protein–dye binding. *Analytical Biochemistry* **72,** 248–254.

Chew O, Whelan J, Millar AH. 2003. Molecular definition of the ascorbate–glutathione cycle in Arabidopsis mitochondria reveals dual targeting of antioxidant defenses in plants. *Journal of Biological Chemistry* **278,** 46869–46877.

Clifton R, Millar AH, Whelan J. 2006. Alternative oxidases in Arabidopsis: a comparative analysis of differential expression in the gene family provides new insights into function of non-phosphorylating bypasses. *Biochimica et Biophysica Acta* **1757,** 730–741.

Del Longo OT, González CA, Pastori GM, Trippi VS. 1993. Antioxidant defences under hyperoxygenic and hyperosmotic conditions in leaves of two lines of maize with differential sensitivity to drought. *Plant and Cell Physiology* **34,** 1023–1028.

Dietz KJ, Jacob S, Oelze ML, Laxa M, Tognetti V, de Miranda SMN, Baier M, Finkemeier I. 2006. The function of peroxiredoxins in plant organelle redox metabolism. *Journal of Experimental Botany* **57,** 1697–1709.

Faske M, Backhausen JE, Sendker M, Singer-Bayrle M, Scheibe R, von Schaewen A. 1997. Transgenic tobacco plants expressing pea chloroplast *Nmdh* cDNA in sense and antisense orientation: effects on NADP-malate dehydrogenase level, stability of transformants, and plant growth. *Plant Physiology* **115,** 705–715.

Faske M, Holtgrefe S, Ocheretina O, Meister M, Backhausen JE, Scheibe R. 1995. Redox equilibria between the regulatory thiols of light/dark-modulated chloroplast enzymes and dithiothreitol: fine-tuning by metabolites. *Biochimica et Biophysica Acta* **1247,** 135–142.

Foyer CH, Halliwell B. 1976. The presence of glutathione and glutathione reductase in chloroplasts: a proposed role in ascorbic acid metabolism. *Planta* **133,** 21–25.

Foyer CH, Noctor G. 2009. Redox regulation in photosynthetic organisms: signalling, acclimation, and practical implications. *Antioxidants and Redox Signaling* **11,** 861–905.

Foyer CH, Bloom AJ, Queval G, Noctor G. 2009. Photorespiratory metabolism: genes, mutants, energetics, and redox signaling. *Annual Review of Plant Biology* **60,** 455–484.

Genty B, Briantais J-M, Baker NR. 1989. The relationship between the quantum yield of photosynthetic electron transport and quenching of chlorophyll fluorescence. *Biochimica et Biophysica Acta* **990,** 87–92.

Giraud E, Ho LH, Clifton R, *et al*. 2008. The absence of ALTERNATIVE OXIDASE1a in Arabidopsis results in acute sensitivity to combined light and drought stress. *Plant Physiology* **147,** 595–610.

Graeve K, von Schaewen A, Scheibe R. 1994. Purification, characterization, and cDNA sequence of glucose-6-phosphate dehydrogenase from potato (*Solanum tuberosum* L.). *The Plant Journal* **5,** 353–361.

Hanke GT, Holtgrefe S, König N, Strodtkötter I, Voss I, Scheibe R. 2009. Use of transgenic plants to uncover strategies for maintenance of redox-homeostasis during photosynthesis. In: Jacquot J-P, ed. *Advances in botanical research: oxidative stress and redox regulation in plants*, Vol. 52. New York: Academic Press, 207–251.

Hare PD, Cress WA, van Staden J. 1999. Proline synthesis and degradation: a model system for elucidating stress-related signal transduction. *Journal of Experimental Botany* **50,** 413–434.

Igamberdiev AU, Bykova NV, Lea PJ, Gardeström P. 2001. The role of photorespiration in redox and energy balance of photosynthetic plant cells: a study with a barley mutant deficient in glycine decarboxylase. *Physiologia Plantarum* **111,** 427–438.

Kangasjärvi S, Lepistö A, Hännikäinen K, Piippo M, Luomala E-M, Aro E-M, Rintamäki E. 2008. Diverse roles of chloroplast stromal and thylakoid-bound ascorbate peroxidases in plant stress responses. *Biochemical Journal* **412,** 275–285.

König J, Baier M, Horling F, Kahmann U, Harris G, Schürmann P, Dietz KJ. 2002. The plant-specific function of 2-Cys peroxiredoxin-mediated detoxification of peroxides in the redox-hierarchy of photosynthetic electron flux. *Proceedings of the National Academy of Sciences, USA* **99,** 5738–5743.

Laisk A, Eichelmann H, Oja V, Talts E, Scheibe R. 2007. Rates and roles of cyclic and alternative electron flow in leaves. *Plant and Cell Physiology* **48,** 1575–1588.

Lee KP, Kim C, Landgraf F, Apel K. 2007. EXECUTER1- and EXECUTER2-dependent transfer of stress-related signals from the plastid to the nucleus of *Arabidopsis thaliana*. *Proceedings of the National Academy of Sciences, USA* **104,** 10270–10275.

Lepistö A, Kangasjärvi S, Luomala E-M, Brader G, Sipari N, Keränen M, Keinänen M, Rintamäki E. 2009. Chloroplast NADPH-thioredoxin reductase interacts with photoperiodic development in Arabidopsis. *Plant Physiology* **149,** 1261–1276.

Lisec J, Schauer N, Kopka J, Willmitzer L, Fernie AR. 2006. Gas chromatography–mass spectrometry-based metabolite profiling in plants. *Nature Protocols* **1,** 387–396.

Liu Y, Ye N, Liu R, Chen M, Zhang J. 2010. H_2O_2 mediates the regulation of ABA catabolism and GA biosynthsis in *Arabidopsis* seed dormancy and germination. *Journal of Experimental Botany* **61,** 2979–2990.

Mullineaux PM, Rausch T. 2005. Glutathione, photosynthesis and the redox regulation of stress-responsive gene expression. *Photosynthesis Research* **86,** 459–474.

Narendra S, Venkataramani S, Shen G, Wang J, Pasapula V, Lin Y, Kornyeyev D, Holaday AS, Zhang H. 2006. The Arabidopsis ascorbate peroxidase 3 is a peroxisomal membrane-bound antioxidant enzyme and is dispensable for Arabidopsis growth and development. *Journal of Experimental Botany* **57,** 3033–3042.

Niyogi KK. 2000. Safety valves for photosynthesis. *Current Opinion in Plant Biology* **3,** 455–460.

Noctor G, Foyer CH. 1998. Ascorbate and glutathione: keeping active oxygen under control. *Annual Review in Plant Physiology and Plant Molecular Biology* **49,** 249–279.

Nunes-Nesi A, Carrari F, Lytovchenko A, Smith AMO, Loureiro ME, Ratcliffe R, Sweetlove LJ, Fernie AR. 2005. Enhanced photosynthetic performance and growth as a consequence of decreasing mitochondrial malate dehydrogenase activity in transgenic tomato plants. *Plant Physiology* **137,** 611–622.

Padmasree K, Raghavendra AS. 1999. Response of photosynthetic carbon assimilation in mesophyll protoplasts to restriction on mitochondrial oxidative metabolism: metabolites related to the redox status and sucrose biosynthesis. *Photosynthesis Research* **62,** 231–239.

Pérez-Ruiz JM, Spinola MC, Kirchsteiger K, Moreno J, Sahrawy M, Cejudo FJ. 2006. Rice NTRC is a high-efficiency redox system for chloroplast protection against oxidative damage. *The Plant Cell* **18,** 2356–2368.

Piippo M, Allahverdiyeva Y, Paakkarinen V, Suoranta U-M, Battchikova N, Aro E-M. 2006. Chloroplast-mediated regulation of nuclear genes in *Arabidopsis thaliana* in the absence of light stress. *Physiological Genomics* **25,** 142–152.

Pulido P, Spínola MC, Kirchsteiger K, Guinea M, Pascual MB, Sahrawy M, Sandalio LM, Dietz KJ, González M, Cejudo FC. 2010. Functional analysis of the pathways for 2-Cys peroxiredoxin reduction in *Arabidopsis thaliana* chloroplasts. *Journal of Experimental Botany* **61,** 4043–4054.

Riazunnisa K, Padmavathi L, Scheibe R, Raghavendra AS. 2007. Preparation of Arabidopsis mesophyll protoplasts with high rates of photosynthesis. *Physiologia Plantarum* **129,** 679–686.

Rius SP, Casati P, Iglesias AA, Gomez-Casati DF. 2006. Characterization of an *Arabidopsis thaliana* mutant lacking a cytosolic non-phosphorylating glyceraldehyde-3-phosphate dehydrogenase. *Plant Molecular Biology* **61,** 945–957.

Scheibe R. 2004. Malate valves to balance cellular energy supply. *Physiologia Plantarum* **120,** 21–26.

Scheibe R, Backhausen JE, Emmerlich V, Holtgrefe S. 2005. Strategies to maintain redox homeostasis during photosynthesis under changing conditions. *Journal of Experimental Botany* **56,** 1481–1489.

Scheibe R, Dietz KJ. 2011. Reduction–oxidation network for flexible adjustment of cellular metabolism in photoautotrophic cells. *Plant, Cell and Environment* (in press).

Scheibe R, Jacquot JP. 1983. NADP regulates the light activation of NADP-dependent malate dehydrogenase. *Planta* **157,** 548–553.

Scheibe R, Stitt M. 1988. Comparison of NADP-malate dehydrogenase activation, Q_A reduction and O_2 evolution in spinach leaves. *Plant Physiology and Biochemistry* **26,** 473–481.

Schreiber U, Schliwa U, Bilger W. 1986. Continuous recording of photochemical and nonphotochemical chlorophyll fluorescence quenching with a new type of modulation fluorometer. *Photosynthesis Research* **10,** 51–62.

Serrato AJ, Pérez-Ruiz JM, Spinola MC, Cejudo FJ. 2004. A novel NADPH thioredoxin reductase, localized in the chloroplast, which deficiency causes hypersensitivity to abiotic stress in *Arabidopsis thaliana*. *Journal of Biological Chemistry* **279,** 43821–43827.

Shen W, Wei Y, Dauk M, Tan Y, Taylor DC, Selvaraj G, Zou J. 2006. Involvement of a glycerol-3-phosphate dehydrogenase in modulating the NADH/NAD^+ ratio provides evidence of a mitochondrial glycerol-3-phosphate shuttle in Arabidopsis. *The Plant Cell* **18,** 422–441.

Sims DA, Gamon JA. 2002. Relationship between leaf pigment content and spectral reflectance across a wide range of species, leaf structures and developmental stages. *Remote Sensing of Environment* **81,** 337–354.

Smyth GK, Yang YH, Speed T. 2003. Statistical issues in cDNA microarray data analysis. *Methods in Molecular Biology* **224,** 111–136.

Spinola MC, Perez-Ruiz JM, Pulido P, Kirchsteiger K, Guinea M, Gonzalez M, Cejudo FJ. 2008. NTRC new ways of using NADPH in the chloroplast. *Physiologia Plantarum* **133,** 516–524.

Strodtkötter I, Padmasree K, Dinakar C, *et al*. 2009. Induction of the AOX1D isoform of alternative oxidase in *A. thaliana* T-DNA insertion lines lacking isoform AOX1A is insufficient to optimize photosynthesis when treated with antimycin A. *Molecular Plant* **2,** 284–297.

Szabados L, Savouré A. 2009. Proline: a multifunctional amino acid. *Trends in Plant Science* **15,** 89–97.

Tomaz T, Bagard M, Pracharoenwattana I, Lindén P, Lee CP, Carroll AJ, Ströher E, Smith SM, Gardeström P, Millar AH. 2010. Mitochondrial malate dehydrogenase lowers leaf respiration and alters photorespiration and plant growth in Arabidopsis. *Plant Physiology* **154,** 1143–1157.

Tripathi BN, Bhatt I, Dietz KJ. 2009. Peroxiredoxins: a less studied component of hydrogen peroxide detoxification in photosynthetic organisms. *Protoplasma* **235,** 3–15.

Walker D. 1988. *The use of the oxygen electrode and fluorescent probes in simple measurements of photosynthesis*. Sheffield: Oxygraphics Ltd.

Wingler A, Lea PJ, Quick WP, Leegood RC. 2000. Photorespiration: metabolic pathways and their role in stress protection. *Philosophical Transactions of the Royal Society B: Biological Sciences* **355,** 1517–1529.

Wilson AK, Pickett FB, Turner JC, Estelle M. 1990. A dominant mutation in *Arabidopsis* confers resistance to auxin, ethylene and abscisic acid. *Molecular Genetics and Genomics* **222,** 377–383.

Yoshida K, Terashima I, Noguchi K. 2007. Up-regulation of mitochondrial alternative oxidase concomitant with chloroplast over-reduction by excess light. *Plant and Cell Physiology* **48,** 606–614.